IMPROVING ESTIMATES OF DEPTH, MAGNITUDE, AND FAULTING PARAMETERS OF EARTHQUAKES IN CENTRAL ASIA

Charles J. Ammon,[1] George E. Randall,[2] and Jordi Julia[1]

Penn State University,[1] Los Alamos National Laboratory[2]

Sponsored by National Nuclear Security Administration
Office of Nonproliferation Research and Engineering
Office of Defense Nuclear Nonproliferation

Contract No. DE-FC04-00AL67668

ABSTRACT

Accurate and stable seismic source parameters for small-to-moderate size events are essential for many aspects of regional nuclear explosion monitoring. For example, magnitude and distance amplitude corrections (MDAC) have been developed for regional discrimination, but they rely on stable moment estimates. We develop a catalog of regional earthquakes in eastern Asia with estimated seismic moments, source mechanisms, and depths using regional seismic data. A significant challenge of modeling small-to-moderate-size seismic sources is the necessity of relying on short-period signals with long travel paths that have substantial sensitivity to earth structure along the path. When the path effects are unknown or difficult to account for, we must rely on components of seismic signals that are minimally dependent on the structure. Although regional surface-wave phases are strongly influenced by structure, surface-wave amplitude spectra can be modeled adequately with relatively simple earth models, and these spectra carry valuable information on source character. Our efforts build on existing seismic source analysis techniques. We directly model regional seismograms where possible but combine those with surface-wave amplitude spectra observed at more distant stations. The inversion is performed using a grid search for strike, dip, rake, moment, and depth. When available, we also include long-period body-wave trains, which can be modeled reliably using simple stratified earth models. The use of spectra and long-period signals is ideal for estimating the moment and faulting geometry of signals but simple least-squares norms based on these signals do not often provide satisfactory resolution of source depth (when the source is shallow). However, in cases where the long-period mechanism is relatively stable as a function of depth, we can overcome this limitation by exploiting signals more diagnostic of source depth such as teleseismic body-waveforms, broad-band Pn waveforms, or select short-period Rayleigh wave spectra. We use an L1 norm for all the modeling, scaling each signal's misfit by the signal power. Once the best mechanism is identified we search for a weighted L1 optimal seismic moment with confidence intervals.

OBJECTIVE

Estimating the source type or faulting geometry of small seismic events located hundreds of kilometers from the nearest seismometer can be difficult. Typically one of two classes of modeling approaches are adopted: Spectral or time-domain. Spectral techniques use the observed variation in surface-wave spectra as a function of azimuth to match the radiation pattern of the source (*e.g.* Patton, 1976, 1980, 1998; Herrmann, 1976, 1979; Romanowicz, 1982; Patton and Zandt, 1992; Herrmann and Ammon, 1997, and many others). Time-domain methods are straight-forward matches to the observed seismograms and include both amplitude and phase information (*e.g.* Langston, 1981; Dreger and Helmberger, 1991, 1992, 1993; Lay et al., 1994; Randall et al., 1995; Ghose et al, 1998; Ammon et al., 1998, and others). Spectral methods can be designed to include amplitude only, or amplitude and phase information, while time-domain methods include both. Phase information provides valuable constraints on the source mechanism and depth, but the observed phase is often sensitive to details in Earth structure along the propagation path. Time-domain source inversion methods are usually applied to large events with good long-period signals or short-period signals of small events that have minimal distortion from Earth structure (such as teleseismic P and SH waves) or local and close-regional (less than a few hundred *km*) signals. To use phase in surface-wave spectral analyses works best with a good estimate of the surface-wave phase velocity variations between the source and receiver.

If we consider the problem addressed in nuclear explosion monitoring, the best signals from a shallow small event are most likely to be short-period surface waves. But directly fitting the phase of short-period Rayleigh waves (probably the best regionally observed, deterministic signal from a small, shallow event) is challenging because these waves are sensitive to shallow, variable structure along the propagation path. Rayleigh-wave spectral amplitudes are less sensitive to structure variations than the corresponding signal phase, and contain valuable information on the source depth. Thus it is desirable to combine the part of distant signals that is less sensitive to structure with the amplitude and phase information from the closer stations.

Simultaneous Spectral and Time-domain Seismic Source Modeling

To achieve this, we combine surface-wave spectral amplitude modeling and time-domain waveform fitting in a grid-search algorithm to estimate the source mechanism (systematically check strike, dip, rake, and depth, & include an isotropic source for comparison). The procedure includes surface-wave amplitude information for all stations and includes both amplitude and phase information from the closer observations (either complete three components or Pnl) and teleseismic body waves if the event is large enough for these to be observed (Figure 1). Incorporating observations from more distant stations makes a significant contribution to seismic source studies in two important ways: First, the azimuthal coverage of radiation patterns is improved and second, Rayleigh wave amplitude spectra contain information on the source depth. For shallow events, improved resolution of the depth requires short-period information because the information on shallow depths are contained in the short-period signals. Herrmann (1979) exploited information in intermediate-period surface waves to estimate the faulting geometry and depth of earthquakes in the east and central North America from old analog records. He observed signals out to distances of thousands of kilometers and extracted spectral amplitudes suitable for constraining the earthquake parameters. Our experience suggests that observations from such large distances in central Asia are not as simple or robust as those in the stable part of North America (*e.g.* Levshin et al.,1990). The signal amplitudes are complicated due to scattering and intrinsic attenuation, but generally well observed for larger events (Mw ~ 5). However, signals from small events may be isolated from background noise and extracted using phase-match filtering exploiting dispersion observations from larger events.

RESEARCH ACCOMPLISHED

The goal of estimating source depth with some precision requires a combination of observations. Particularly valuable in constraining earthquake depth are short-period Rayleigh waves, which may contain a spectral notch indicative of source depth (e.g. Herrmann, 1979) but often shown systematic amplitude variations that vary with depth. Short-period surface waves can be tricky and when analyzing the signals some form of mode isolation can help simplify their interpretation. Currently we use group velocity windows with spectral smoothing to simplify the seismic signals, but preliminary studies of the impact of mode isolation indicates that it is often not necessary for

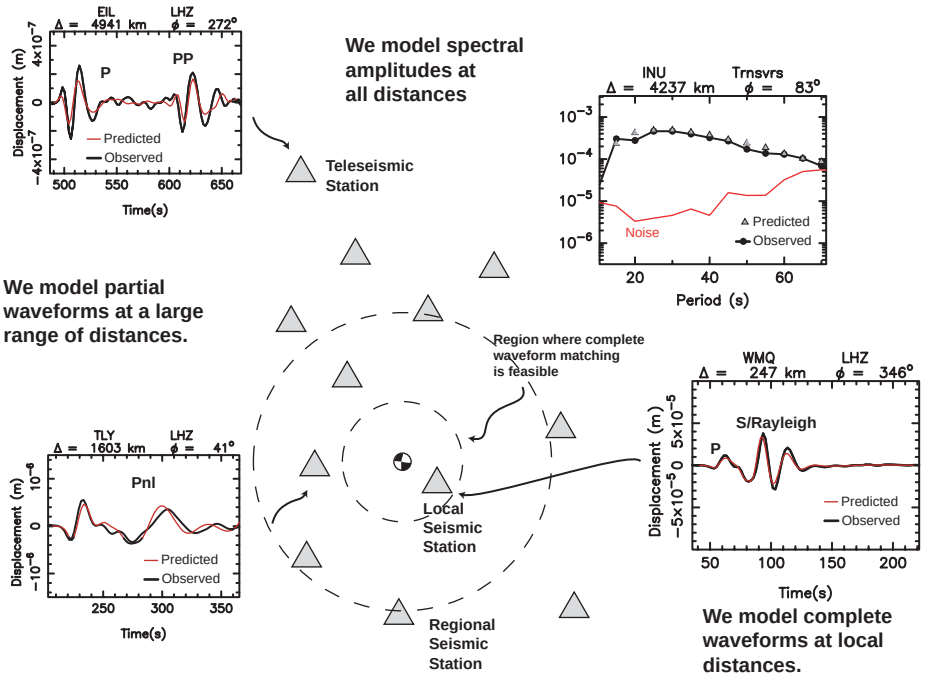

Figure 1. Schematic illustration of the joint source parameter inversion scheme. The triangles represent seismic stations, the focal mechanism represents the source location. The basic idea is to combine observations with a minimal sensitivity to earth structure to produce more accurate estimates of the event mechanism and depth. Since most observations are too far for direct short-period waveform modeling we sacrifice the phase information and use only the more robust spectral amplitudes at those sites. Phase information is included from seismograms recorded at nearby stations, teleseismic P-waves, or regional *Pnl* arrivals. Sample observations and predictions are shown around the margins.

larger events - or it adds little improvement. That may not be the case when event signals are small and separation from background noise requires some form of signal enhancement.

Our primary control on the source mechanism arises from the azimuthal variation of Rayleigh and Love wave spectra. Nearby time-domain signals provide the required phase information as well as additional information on the mechanism and often the most sensitivity to depth. All spectra are estimated using a windowed autocorrelation function which produces smoother and statistically more reliable spectral amplitudes. This procedure requires substantially more time than using the FFT amplitude spectrum since the smoothing requires that we incorporate periods adjacent to those used in the misfit norm. However, the smooth, statistically-better measures should be more valuable for analyses of path effects and systematic variations in signals at particulate stations. The seismic moment for each mechanism tested in the grid search is estimated using an L1 fit to the logarithm of spectral amplitudes of all the signals. Green's functions are computed using a generic model of a slightly thicker than average (46 km) continent resting on an earth-flattening transformed version of the isotropic Preliminary Reference Earth Model (PREM).

Our early inversions revealed that many of the data available from the global seismic networks are noisy or contain other problems that render them unsuitable for use in an inversion. To identify a problem, we visually inspect all the data in the bandwidth from 100 to 20 seconds period to identify signals with grossly inadequate signal-to-noise ratios. To insure that we rely more heavily on the best observations, we weight each spectral observation by the inverse of the ambient seismic noise at the same period. The ambient noise is estimated using the pre-P-wave signal. Each signal's spectrum is also weighted relative to all other spectra using the mean of spectral amplitude of the noise in the period range of interest. Distant stations are down-weighted using a simple one-over-distance measure. This is strictly a pragmatic approach designed to include our *a priori* assumption that the model we are using is probably best suited

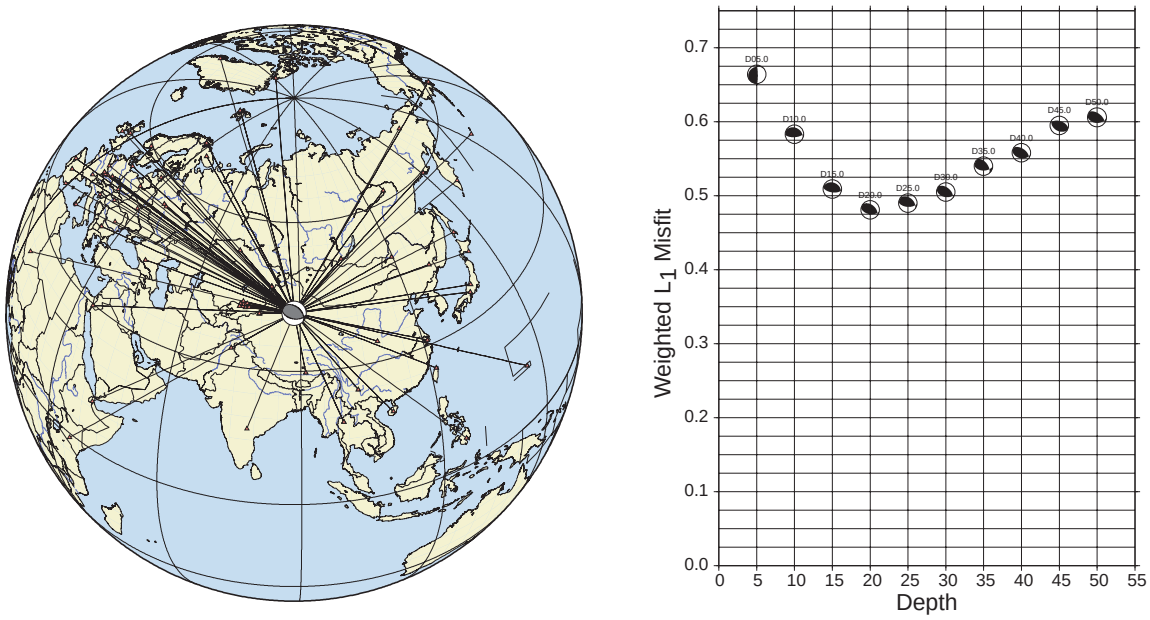

Figure 2. Sample inversion results for event with Harvard ID B013099A. The paths from the source to the station are shown on the left, the mechanisms on the right are plotted on the right. The best depth is 20 km but solutions at 25 km are also acceptable. Sample observed-predicted fits were used to illustrate the inversion ideas in Figure 1.

for short paths. Interestingly, we have found little correlation of misfits with distance, suggesting that we are able to fit the most distant observations with the same fidelity that we fit the intermediate distance observations. Azimuthal bias in station coverage is moderated by weighting observations by the number of other signals within 15° azimuthal range of the particular observation. In other words, a signal separated from all others by a gap of more than 15° has an azimuthal weight of 1.0 and a signal with 4 other signals within 15° has an azimuthal weight of 0.2 (1/5, including the observation). Automating the weights substantially reduces the time needed to adjust the parameters during an inversion. Observation weights reflect our attempts to cope with the problems of driving an inversion with a single-number norm.

Although each event is different, the combination of these observations can produce good depth, mechanism, and seismic moment constraints. Data coverage and results for an example inversion are shown in Figure 2. The event was located in Southern Xinjiang, China and occurred on 1999 01/30 03:51:5.00. This inversion included 123 signals, including 3 complete seismograms recorded at nearby station WMQ, 10 vertical component P-waveforms, 2 radial component Pnl waveforms, 71 Rayleigh-wave spectra, and 37 Love-wave spectra. We fit just over 50% of the power in the weighted signals (visually the fits are very good). The estimated depth is 20 km, the seismic moment is 1.02e24 (M_W = 5.3), and the mechanism corresponds to roughly north-south compression with a near-vertical tension axis. The variation in the complete norm shown in Figure 2 does not necessarily reflect the variation in fit to just the time-domain signals. To identify such instances we track 8 norms: vertical-radial complete- and partial-waveform seismogram misfits, Rayleigh-wave spectral misfits, transverse component complete seismogram misfit and Love-wave spectral misfit, and the combination of all misfits (that was used in Figure 2).

Uncertainties

We have investigated two approaches to quantifying uncertainties. For seismic moment uncertainty, we estimate the weighted L1 misfit optimal moment using a grid search employing the best fitting dislocation. A by product of the grid search is a moment versus misfit curve (Figure 3). Note the strong asymmetry in the misfit versus moment curve.

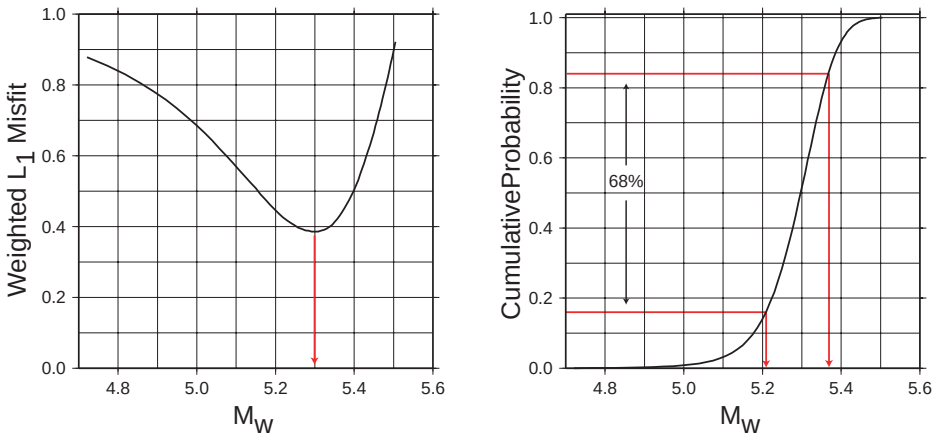

Figure 3. Moment versus weight, L1 misfit is shown on the left and a cumulative probability distribution derived from the misfit curve is shown on the right. The red lines indicate the range containing 68% of the probability around the best fitting solution (the same area associated with one standard deviation). The asymmetry in the misfit curve is reflected in asymmetry in the confidence range.

This is a consequence of misfit arising from a number of non-simple sources, including Green's function inadequacy, background seismic noise, *etc.* We can estimate a confidence interval using the misfit curve if we can estimate the equivalent of a standard deviation in the observations. Based on experience with different velocity models, propagation geometries, etc., we assumed a value of 0.1 for an effective absolute deviation width normalization constant (an equivalent of a "standard deviation"). With this value defined, we can map the misfits into an exponential likelihood function, which we can integrate as shown on the right in Figure 3.

We can identify various likelihood values on the curve and estimate ranges for different confidence intervals. For the example event (optimal $M_W = 5.3$), we found a 68% confidence range in M_W was 5.20 to 5.36; a 95% confidence range of 5.07 to 5.43; and a 99% confidence range of 4.82 to 5.48. The single-standard deviation equivalent range of 0.1 lower and 0.06 higher is relatively good and equivalent to errors calculated from large-size Harvard CMT solutions. The larger values on the more demanding confidence intervals grow to the point where you can see differences in all of the observed-predicted comparisons. We believe that these numbers include the effects of assuming what different models would have on the results, this scales the misfit by 0.1 when mapping into a likelihood function.

To estimate uncertainties in the dislocation parameters, we explore the variation in individual misfit measure such as vertical, radial, transverse seismograms and vertical and transverse spectra, into separate norms. We use a multiple-objective optimization (MOO) approach to identify the solutions optimal for each of our tracked misfit norms. The MOO framework allows the identification of solutions that bound the region of feasible solutions (Ammon, 2003). A two-dimensional example is illustrated in Figure 4 and 5. Figure 4 is a map of dislocation misfits for the case of seismograms and spectral split into two separate norms. A search for solutions that are not dominated by other solutions (no other solution has a lower misfit in at least one of the two norms for the solutions). The non-dominated solutions form the boundary surrounding the range of feasible solutions. They are shown in red in Figure 4. The mechanisms associated with the non-dominated solution are shown in Figure 5. Most solutions are roughly east-west reverse fault with one exception. The exception corresponds to the best fitting solution for amplitude spectra only. The inclusion of any information on time-domain signals eliminates this solution from serious consideration, but the example illustrates the short-comings of inversions without phase information. Formally, this solution produces amplitude spectra very similar to those of the other mechanisms. The lack of phase information allows a 90° rotation of the tension axis with little change in the amplitude spectra. The Pareto solutions span a depth range of 15-25 km, but the range narrows to 20-25 km as soon as we consider seismogram misfits. The moment magnitude for all the solutions is 5.3 and the estimated uncertainties were discussed earlier. Our preferred solution is that closest to the ideal solution (shown in blue in Figure 4). This is the dislocation is the closest to best fitting both data sets which we

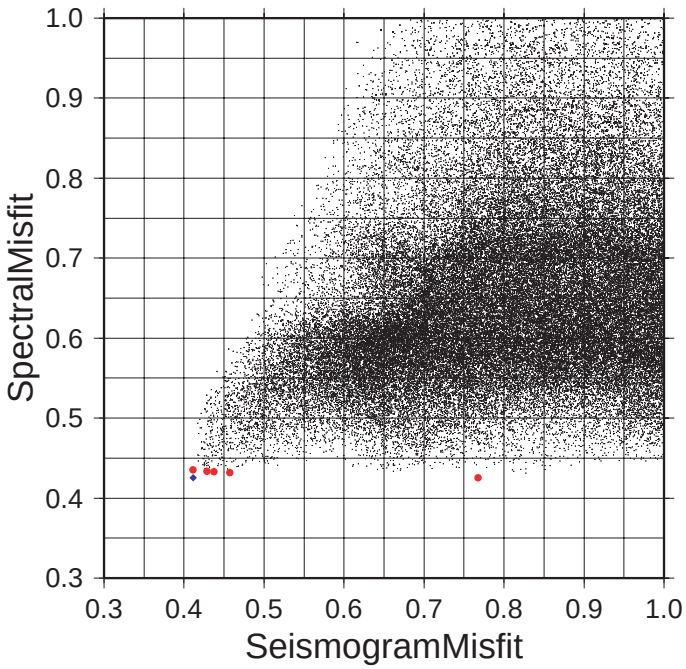

Figure 4. Two-dimensional objective space created by combining all of our time-domain misfits and our spectral amplitude misfits into two norms. The misfits associated with each dislocation are shown as black points. The blue point identifies the ideal solution (the ideal solution identified with the lowest value in each norm). The red points show the Pareto set, solutions not dominated by any other solutions. The Pareto solution far to the right is associated with the best norm for the amplitude spectra, but does not fit the seismograms.

can fit either independently. In this case the solution has a strike, dip, and rake of 310, 40, 120, respectively, and a depth of 20 km.

Joint Amplitude-Spectra/Seismogram Grid-Search Inversion Results

Preliminary grid-search results are shown in Figure 6. In general our results agree with the Harvard mechanisms, although often some rotation of the mechanisms is required by our data and occasionally we appear to have less control on the mechanism. Perhaps the most interesting difference is the dependence of the seismic moment difference between Harvard and our analyses on seismic moment. For moderate-size events ($M_W > 5.5$) our moments agree well with Harvard's, for events near the threshold of the CMT method, more often than not the Harvard CMT moment is larger than the moments derived by us (Figure 7). No doubt some of the difference arises from the different models used in each method and our moment is really a fit of the spectrum from 80 to 20 seconds, for the smaller events, Harvard's moment is generally more appropriate near 40 seconds period (when only body waves are used). Most interesting is the character of the discrepancy which suggests a systematic difference as a function of moment. For the smaller magnitude events, the misfit is substantial when inspecting the time-domain signals. All events with a grid-search moment magnitude less than 5.0 are produce positive residual magnitudes (which indicates overestimation by Harvard or underestimation by us). Such differences may reflect the excitation functions for the different velocity structures assumed in each method, and while they cannot be resolved completely (moment depends on the assumed structure), the differences can be important are worth noting.The moment-magnitudes obtained from the two waveform modeling techniques agree better than either does with Ms. A comparison of the grid-search M_W and the USGS Ms is shown in Figure 7. For simplicity, we've assumed the same uncertainty in grid search M_W as exists in the Harvard CMT solution. Here the trend is the opposite with M_S for smaller events under-predicting their size. The trend is unchanged if you use the Harvard CMT moments - the differences are larger.

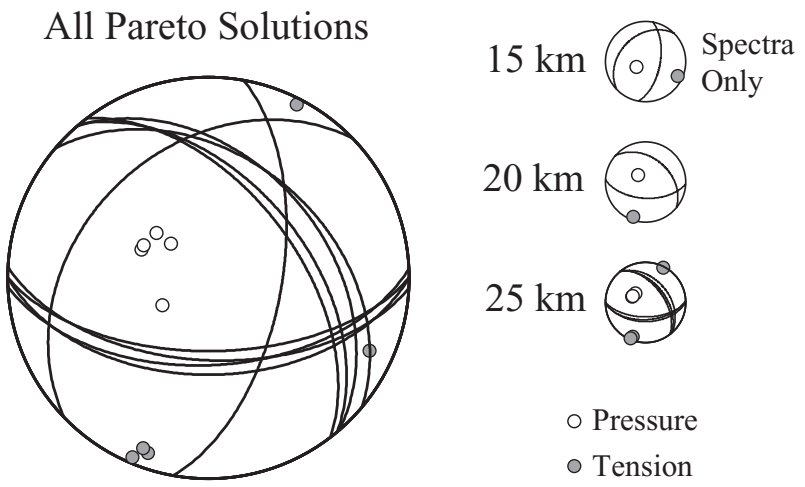

Figure 5. Pareto solutions for the example inversion. The mechanisms cluster tightly with one exception. The "outlier" solution corresponds to the lowest amplitude spectral misfit. The lack of phase information allows a 90° rotation of the T axis and still produces a good fit. The other solutions include amplitude and phase information and correspond to the preferred solution.

CONCLUSIONS AND RECOMMENDATIONS

The addition of teleseismic body waves directly into the inversion will also help refine the depths of the larger events for which the body-wave signals are adequate. It may be possible to simply use the teleseismic to estimate depth, fixing the moment and mechanism from the spectra and regional seismograms. Then a relatively easy-to-implement cross-correlation misfit norm, which requires little effort on aligning the signals, could be used to estimate the depth. For the shallowest events, inspection of short-period surface waves from nearby stations may help confirm source depth and add important confidence to the grid-search results. Such additional information is subjective but there may be no likely way to avoid classifying solution quality without some fuzziness. Seismic signals are complex and their sensitivity to different aspects of the source are difficult to quantify with easily computed misfit norms.

ACKNOWLEDGEMENTS

We thank the P. Wessel and W. H. F. Smith, the authors of GMT for producing easy-to-use, quality software for making maps and charts and T. J. Pearson, author of PGPLOT library, for producing a robust, flexible, well-documented graphics library.

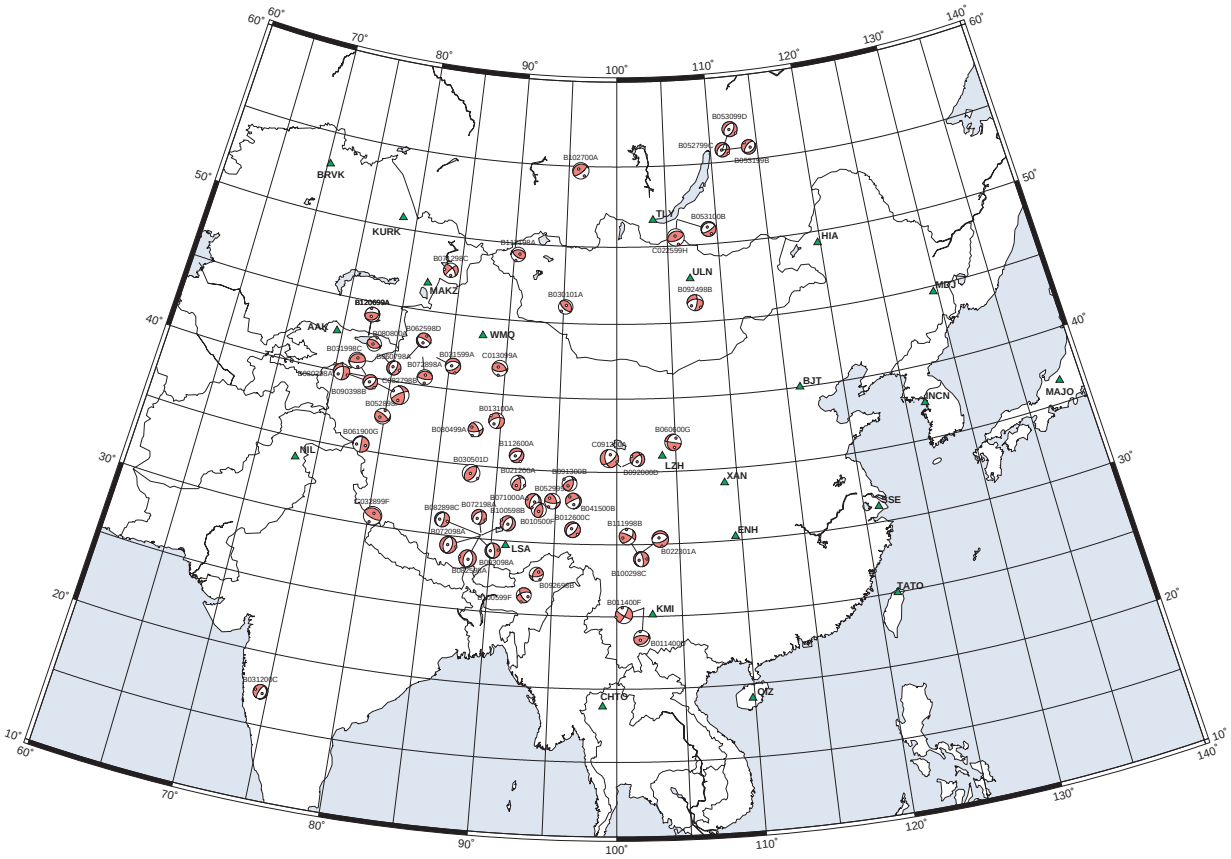

Figure 6. The map above shows the results of inversions using the waveforms and spectra for 30 events in the Harvard CMT Catalog. The results are generally consistent although some of our mechanisms have significant rotations relative to the CMT solutions (and what you might expect from tectonics). We believe that part of the problem with our preliminary results lies in the use of small-amplitude signals. Our seismic moments (or Mw) are less sensitive to variations in structure and noisy traces (for these inversions we used the L1 norm and the median values to compute an optimal moment in the period range from 65 to 20 s). For some events, no nearby waveforms are available and the results are ambiguous (but constrained) - for example, the rake can be changed by $\pm\pi$.

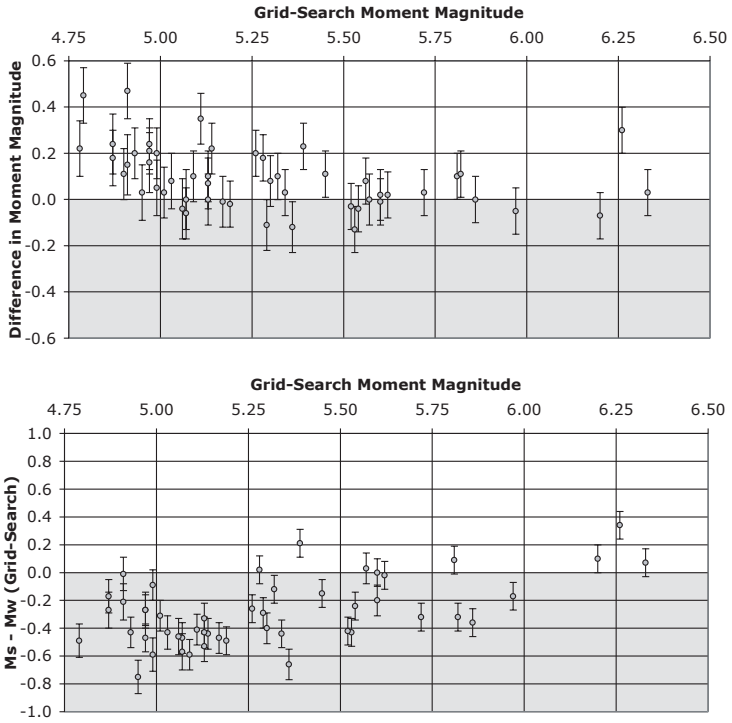

Figure 7. (Top) Comparison of the moment from grid searches and the Harvard CMT moment. Vertical axis shows the (Harvard Mw) – (Grid-Search Mw). Since the two approaches use different velocity structures and fit the data over different, finite bandwidths, the agreement should not be perfect. The CMT method tends to over-predict (or our method under-predicts) the moment for small events. Uncertainties were computed for the Harvard CMT using a Monte-Carlo method. The outlier at Mw 6.25 is a result of our failure to incorporate a time function for this larger event (Mw > 6.5). (Bottom) Comparison of the moment magnitude from grid searches and the USGS Ms estimate. Vertical axis shows the (Ms) – (Grid-Search Mw). Uncertainties were computed for the grid-search were computed using a Monte-Carlo method on the CMT moments (an approximation).

REFERENCES

Ammon, C. J., Seismic Source Inversion as a Multiple Objective Optimization Problem, submitted to Geophysical Journal International (under revision), 2003.

Ammon, C. J., R. B. Herrmann, C. A. Langston and H. Benz (1996), Source parameters of the January 16, 1994 Wyomissing Hills, Pennsylvania earthquakes, Seism. Res. Letters, 69, 261-269.

Dreger, D. S., and D. V. Helmberger (1990), Complex faulting deduced from broadband modeling of the 28 February 1990 Upland Earthquake, Bull. Seism. Soc. Am., 81, 1129-1144.

Dreger, D. S., and D. V. Helmberger (1991), Source Parameters of the Sierra Madre earthquake from regional and local body waves, Geophys. Res. Letters, 18, 2015-2018.

Dreger, D. S., and D. V. Helmberger (1993), Determination of source parameters at regional distances with three-component sparse network data, J. Geophys. Res., 98, 8107-8125.

Ghose, S., M. W. Hamburger and C. J. Ammon (1998), Source parameters of moderate-size earthquakes in the Tien Shan, central Asia from regional moment tensor inversion, Geophys. Res. Letters, 25, 3181-3184.

Herrmann, R. B. (1979), Surface wave focal mechanisms for eastern North American Earthquakes with tectonic implications, J. Geophys. Res., 84, 3543-3552.

Herrmann, R. B. (1986), Surface-Wave studies of some South Carolina earthquakes, Bull. Seism. Soc. Am., 76, 111-121.

Langston, C. A. (1981), Source inversion of seismic waveforms: the Koyna, India, Earthquakes of 13 September, 1967, Bull. Seism. Soc. Am., 71, 1-24.

Lay, T., C. J. Ammon, A. A. Velasco, J. Ritsema, T. C. Wallace and H. J. Patton (1994), Near-real time seismology: Rapid analysis of earthquake faulting, GSA Today, 4, 129,132-134.

Levshin, A., L. Ratnikova and J. Berger (1992), Peculiarities of surface-wave propagation across central Asia, Bull. Seism. Soc. Am., 82, 2464-2493.

Patton, H. (1976), A note on the source mechanism of the southeastern Missouri earthquake of October 21, 1965, J. Geophys. Res., 81, 1483-1486.

Patton, H. (1980), Reference point equalization method for determining the source and path effects of surface waves, J. Geophys. Res., 85, 821-848.

Patton, H. J. (1998), Bias in the centroid moment tensor for central Asian earthquakes: Evidence from regional surface wave data, J. Geophys. Res., 103, 26,963-26,974.

Patton, H. J., and G. Zandt (1992), Seismic moment tensors for western U. S. earthquakes and implications for the tectonic stress field, J. Geophys. Res., 96, 18,245-18,259.

Randall, G. R., C. J. Ammon and T. J. Owens (1995), Moment-tensor estimation using regional seismograms from a Tibetan Plateau portable network deployment, Geophys. Res. Letters, 22, 1665-1668.

Romanowicz, B. A. (1982), Moment tensor inversion of long-period Rayleigh Waves: A new approach, J. Geophys. Res., 87, 5395-5407.